中國機械工程學刊第四十二卷第四期第 423~437 頁(民國一百一十年)
Journal of the Chinese Society of Mechanical Engineers, Vol.42, No.4, pp. 423~437 (2021)

Supersonic Flow Around Asymmetrical Cone of Arbitrary Cross Section at High Temperature

Mohamed Roudane*, Toufik Yahiaoui** and Toufik Zebbiche**

Keywords：Cone. Arbitrary cross section. Incidence angle. High temperature. Calorically imperfect gas. Runge Kutta Method. Air. Aerodynamic force. Aerodynamic moment. Normal Shock. Oblique Shock. Conical Shock.

ABSTRACT

The aim of this work is to develop a new numerical model for calculating a supersonic flow and shock parameters around a 3D cone of arbitrary cross-section at high temperature, below the dissociation threshold of the molecules. The developed method consists to divise the cross section at several points, and considering the calculation of the conical shock parameters, as well as the cone surface parameters in each obtained transverse deviation. The flow deviation along each obtained surface is a function of the incidence angle and the inclination formed by this deflection. The flow parameters calculation on the cone surface is done by solving a system of three coupled differential equations with initial condition by the Runge Kutta method. The calculation of the thermodynamic parameters through the conical shock in each transverse direction is made by solving a modified oblique shock wave equations at high temperature. The flow calculation accuracy depends on the discretization of the cross-section. The computation of the aerodynamic force and moment on the cone surface is done consequently, giving each three components in the three directions of the movement. The application is for air.

INTRODUCTION

The supersonic flow around a 3D cone of arbitrary cross-section is particularly important and a practical field in the aeronautical applications for the construction of future missiles and military aircraft, having a strong maneuverability that is easily found for asymmetrical 3D constructions. This construction area will give rise to an aerodynamic force in all three directions that will still produce an aerodynamic moment in the three flight directions, resulting six components of aerodynamic forces. In order to build such machines, we must study the supersonic flow around a cone of arbitrary cross-section of any kind to meet our needed construction. The problem presents a real three-dimensional flow problem. It can be solved by the use of the five conservation equations.

The cone shape at the leading edge is very interesting to study the problem of an attached shock wave. (Maccoll, 1937) presents the circular conical shock wave calculation. This work is valid only at low M_1 which can go to about 2.00. (Kopal, 1947, 1949) presented an aerothermodynamic table giving conical shock parameters using the model presented in (Maccoll, 1937). (Maslen, 1952) studied a supersonic flow around a cone of circular section by CFD equations. (Sims, 1964) illustrates a table by presenting all the physical parameters of a supersonic flow around a right cone of circular section with zero incidences. This study presents a summary of the works presented in (Maccoll, 1937), (Kopal, 1947, 1949) and (Maslen, 1952). (Briggs, 1960) presented a supersonic flow around an elliptical section cone using Laplace's potential velocity equation managing a supersonic flow when M_1<2.00, and θ_C<20°. He took a circle section so that he could use Laplace's equation. (Ndefo, 1969) presents a numerical flow calculation around an asymmetric cone with zero incidence by using CFD in the context of a callorically and thermally *PG*.

(Amidon, 1985) have redone the work presented in (Briggs, 1960) by illustrating all the flow parameters, since in (Briggs, 1960), the results are presented only for *M* and *P*. (Eastman and Omar, 1965) always presented the flow around a straight circular cone by the inverse method.

(Chen and Li, 2000) presented a supersonic flow around a curved cone of circular section. The added value is that the flow can have a compression or an expansion according to the local flow deviation from

Paper Received January, 2020. Revised March, 2021, Accepted March 2021, Author for Correspondence: Toufik Zebbiche.
Email : z_toufik270169@yahoo.fr

**Professor, Department of Mechanical Engineering, Faculty of Technology, University of Blida 1, BP 270 Blida 09000, Algeria.*

***Professor, Institute of Aeronautics and Space Studies, University of Blida 1, BP 270 Blida 09000, Algeria.*

the upstream flow. If a compression is found during the flow, a local shock wave and a decrease in the Mach number is observed. If an expansion of the Prandtl Meyer is found, a local expansion wave and an increase of a local Mach number is observed.

The studies presented in the said (Maccoll, 1937), (Kopal, 1947, 1949), (Maslen, 1952), (Sims, 1964), (Briggs, 1960), (Ndefo, 1969), (Amidon, 1985), (Eastman and Omar, 1965) and (Chen and Li, 2000) are limited only for the calorically and thermally *PG* model, giving well results only if M_1<2.00, T_0<240 K and θ_C<20° for limited application area that does not meet current flight requirements.

(Elaichi and Zebbiche, 2018) developed a new model for calculating the conical shock around a straight circular cone at *HT*, below the dissociation threshold of the molecules, when M_1, T_0 and θ_C are quite high which can reach respectively 6.00, 3500 K and 60° (depending on the attached shock model). This study is presented as a generalization of the works presented in (Maccoll, 1937), (Kopal, 1947, 1949), (Maslen, 1952), (Sims, 1964), (Briggs, 1960), (Ndefo, 1969), (Amidon, 1985), (Eastman and Omar, 1965) and (Chen and Li, 2000). The main difference between (Chen and Li, 2000) and (Maccoll, 1937), (Kopal, 1947, 1949), (Maslen, 1952), (Sims, 1964), (Briggs, 1960), (Ndefo, 1969), (Amidon, 1985) and (Eastman and Omar, 1965) is in the energy equation, where the C_P is taken as constant in (Maccoll, 1937), (Kopal, 1947, 1949), (Maslen, 1952), (Sims, 1964), (Briggs, 1960), (Ndefo, 1969), (Amidon, 1985) and (Eastman and Omar, 1965) and is taken as $C_P(T)$ in (Maccoll, 1937), (Kopal, 1947, 1949), (Maslen, 1952), (Sims, 1964), (Briggs, 1960), (Ndefo, 1969), (Amidon, 1985), (Eastman and Omar, 1965) and (Chen and Li, 2000). This change gives a considerable modification in the mathematical model, and which results in the correction of the results and widening of the field of application.

For air, one finds in (Mc Bride, Gordon and Reno, 1993), (Peterson and Hill, 1965) and (Zebbiche and Youbi, 2007) a series of tabulated values of $C_P(T)$ between 55 K and 3550 K (temperature limit to avoid dissociation). Then, we made an interpolation by a 9th polynomial degree giving a maximum error lower than 0.01% for any temperature.

The aim of this work is to develop a new mathematical model for calculating the shock parameters of a supersonic flow with incidence around a cone of *arbitrary cross-section at HT*, less than the dissociation threshold of the molecules, meeting the current and future need to have flying supersonic military gears with a very strong maneuverability, and in a high M_1 and T_0, which can go to 6.00 and 3500 K respectively as a correction to the results given by the *PG* model of (Maccoll, 1937), (Kopal, 1947, 1949), (Maslen, 1952), (Sims, 1964), (Briggs, 1960), (Ndefo, 1969), (Amidon, 1985), (Eastman and Omar, 1965) and (Chen and Li, 2000), and to the current aerospace constructions witch use a circular section for machines in front of a supersonic flow (Peterson and Hill, 1965) and (Tatum, 1997). The problem therefore consists in determining a mathematical model and developing a new numerical calculation program making it possible to determine the flow parameters θ_S, M_2, P_2/P_1, T_2/T_1, ρ_2/ρ_1, ψ, P_{02}/P_{01} through the conical shock such, isentropic parameters P_2/P_{02}, T_2/T_0, ρ_2/ρ_{02} after the shock and the thermodynamic parameters on the cone surface M_C, T_C/T_0, P_C/P_{02}, ρ_C/ρ_{02}. All these results are a function of θ_C which is also function of the angular deviation β of the lateral surface of the considered 3D cone. Consequently, the aerodynamic force and moment applied on the cone lateral surface can be determined. The application is made for air.

DISCRETIZATION AND FLOW ANGLE DEVIATION

The first step is to discretize the cross section in several points as shown in figure 1. The transverse cone shape is arbitrarily taken. We obtain a series of planes that make angles θ_{Ci} between the deflections of M_1 witch makes an incidence angle α with the reference axes of calculation.

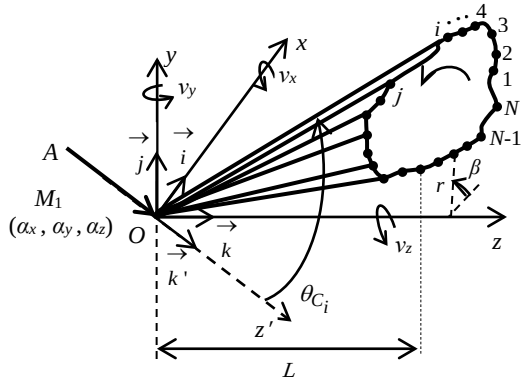

Fig. 1 Cone 3D presentation

The cone is assumed to be in the *Oz* direction, so that the leading edge is originally set to *O*(0,0,0). Then its cross section is parallel to the *xOy* plane. It should be divided into *N* points as shown in figure 1. Then (x_i, y_i, z_i) i=1, 2, ..., *N* are known and differ from one section to another. The numbering of the nodes is done counterclockwise,

$$z_i = L \tag{1}$$

As a result, *N* segments are connected with the point *O* to form *N* triangular elementary surfaces. The numbering of the segment takes the number of the left node for an observer placed at point *O* in the *Oz* axis direction. In each point of the cross section, there is a cone to be considered. The flow calculation in this direction is assimilated to the flow around a cone

of circular section having the same inclination as this plane.

The determination of (x, y, r and β) in all points of the cross section is necessary. Then, the coordinates (x_i, y_i) of point i (i=1, 2, ..., N) of the figure 1 is calculated by,

$$x_i = r_i \cos(\beta_i) \tag{2}$$

$$y_i = r_i \sin(\beta_i) \tag{3}$$

All points i will be linked with the point O to form the chosen cone. The angle β_i is discretized in the viewing interval with respect to the point O.

The Mach number M_1 makes an angle of incidence $\alpha(\alpha_x, \alpha_y, \alpha_z)$ respectively with the coordinate axes Ox, Oy and Oz as shown in the figure 1. Then the flow angle deviation θ_{Ci} of the cone surface number i can be calculated by the following relation,

$$\vec{AO} \wedge \vec{Oi} = \left| \vec{AO} \right| \left| \vec{Oi} \right| \cos\left(\vec{AO}, \vec{Oi} \right) \tag{4}$$

With,

$$\begin{aligned} \vec{AO} &= M_1 \left(\cos\alpha_x \ \vec{i} + \cos\alpha_y \ \vec{j} + \cos\alpha_z \ \vec{k} \right) \\ &= M_1 \ \vec{k}' \end{aligned} \tag{5}$$

And,

$$\vec{Oi} = x_i \ \vec{i} + y_i \ \vec{j} + z_i \ \vec{k} \tag{6}$$

$$\left(\vec{AO}, \vec{Oi} \right) = \theta_{C_i} \tag{7}$$

Which give,

$$\theta_{C_i} = a\cos\left(\frac{\cos\alpha_x \ x_i + \cos\alpha_y \ y_i + \cos\alpha_z \ z_i}{\sqrt{x_i^2 + y_i^2 + z_i^2}} \right) \tag{8}$$

The relation (8) determines the deviation of the section number i of the cone with the upstream velocity vector. This section makes an angle β_i with the positive Ox axis.

One can determine a relation between the angles v and α (figure 1) by the following way. The $Ox'y'z'$ mark is obtained from the $Oxyz$ mark by rotation respectively of the angles v_x, v_y and v_z around the axes Ox, Oy and Oz. While the angles that form M_1 with the axes Ox, Oy and Oz are respectively α_x, α_y and α_z.

The reference $Oxyz$ is provided by the unit vectors $\vec{i}$, $\vec{j}$, $\vec{k}$ and the reference $Ox'y'z'$ is provided by the unit vectors $\vec{i}'$, $\vec{j}'$, $\vec{k}'$. The relationship between the two landmarks is given by,

$$\begin{bmatrix} \vec{i'} \\ \vec{j'} \\ \vec{k'} \end{bmatrix} = [A] \begin{bmatrix} \vec{i} \\ \vec{j} \\ \vec{k} \end{bmatrix} = \begin{bmatrix} A_{11} & A_{12} & A_{13} \\ A_{21} & A_{22} & A_{23} \\ A_{31} & A_{32} & A_{33} \end{bmatrix} \begin{bmatrix} \vec{i} \\ \vec{j} \\ \vec{k} \end{bmatrix} \tag{9}$$

With,

$$[A] = \begin{bmatrix} 1 & 0 & 0 \\ 0 & C_x & S_x \\ 0 & -S_x & C_x \end{bmatrix} \begin{bmatrix} C_y & 0 & S_y \\ 0 & 1 & 0 \\ -S_y & 0 & C_y \end{bmatrix} \begin{bmatrix} C_z & S_z & 0 \\ -S_z & C_z & 0 \\ 0 & 0 & 1 \end{bmatrix} \tag{10}$$

And,

$$C_x = \cos v_x \ , \ C_y = \cos v_y \ , \ C_z = \cos v_z \tag{11}$$

$$S_x = \sin v_x \ , \ S_y = \sin v_y \ , \ S_z = \sin v_z \tag{12}$$

Witch gives,

$$A_{11} = C_y C_z \tag{13}$$

$$A_{12} = C_y S_z \tag{14}$$

$$A_{13} = S_y \tag{15}$$

$$A_{21} = -S_x S_y C_z - C_x S_z \tag{16}$$

$$A_{22} = -S_x S_y S_z + C_x C_z \tag{17}$$

$$A_{23} = S_x C_y \tag{18}$$

$$A_{31} = -C_x S_y C_z + S_x S_z \tag{19}$$

$$A_{32} = -C_x S_y S_z - S_x C_z \tag{20}$$

$$A_{33} = C_x C_y \tag{21}$$

As M_1 is chosen directed along the axis Oz', then by identification of the relations (5) and (9), we can write the following result,

$$\cos \alpha_x = A_{31} \tag{22}$$

$$\cos \alpha_y = A_{32} \tag{23}$$

$$\cos \alpha_z = A_{33} \tag{24}$$

Relationships (22), (23) and (24) can be replaced in relation (8) to determine a relation of θ_C directly as a function of v_x, v_y and v_z.

To determine the values of (v_x, v_y, v_z) as a function of (α_x, α_y, α_z), consider the following system:

. $f_1(v_x,v_y,v_z) = \cos\ \alpha_x - A_{31} = 0$ (25)

$f_2(v_x,v_y,v_z) = \cos\ \alpha_y - A_{32} = 0$ (26)

$f_3(v_x,v_y,v_z) = \cos\ \alpha_z - A_{33} = 0$ (27)

The numerical techniques used to solve a system of nonlinear equations (Raltson and Rabinowitz, 1985) are based on the Jacobian computation; witch is formulated from the derivative of f_1, f_2 and f_3. The numerical tests by using thoses methods demonstrate that the determinant of this Jaconian (denominator of our computation), takes a null value during the computation whatever the chosen initial vector, which interrupts immediatly the calculation. For this reason and to find a solution to our problem, we propose a new fast and robust technique. It converges towards the desired solution without failure.

Physically, the solution (v_x, v_y, v_z) belongs to the interval ([0°, 360°], [0°, 360°], [0°, 360°]).

In the first step, this interval is divided into 4 intervals [90°(l-1), 90°l] l=1, 2, 3 and 4. We calculate the minimum of the maximum in absolute value of f_1, f_2 and f_3 in all points (v_x, v_y, v_z) by a step of one degree with the following relation,

$$f_{Min} = Min\left\{Max\left(\left|f_1\right|,\ \left|f_2\right|,\ \left|f_3\right|\right)_{i,j,k}\right\} \quad (28)$$

With,

$$v_{x_i} = 90\,(l\,\text{-}\,1) + i \qquad i = 0,1,2,...,\ 90 \quad (29)$$

$$v_{y_j} = 90\,(l\,\text{-}\,1) + j \qquad j = 0,1,2,...,\ 90 \quad (30)$$

$$v_{z_k} = 90\,(l\,\text{-}\,1) + k \qquad k = 0,1,2,...,\ 90 \quad (31)$$

And,

$$l = 1, 2, 3, 4 \quad (32)$$

The determined solution (v_x, v_y, v_z) is given with an error in the first digit before the decimal point.

The second step is to determine the solution with an error in the first digit after the decimal point. We look for the solution now in the intervals [v_x-τ, v_x+τ], [v_y-τ, v_y+τ] and [v_z-τ, v_z+τ] for τ=1.0 degree and a step of Δv=0.1 degree with the same way presented in the first step. The determination of the root with an error in the n^{th} digit after the decimal point will be carried out by the choice of $\tau=10^{-n+1}$ degree and a step $\Delta v=\tau/10$ degree.

SHOCK PARAMETERS

The second step is to determine the isentropic parameters (T_1/T_0, ρ_1/ρ_{01}, P_1/P_{01}) corresponding to M_1 and T_0 just before the shock using (33) to (38) (Tatum, 1997) and (Zebbiche, 2009). The relation (33) gives a nonlinear algebraic equation with unknown T_1 which will be determined by the use of the dichotomy algorithm (Raltson and Robinowitz, 1985). Integral (37) is made using Simpson's quadrature with condensation of nodes (Elaichi and Zebbiche, 2018), (Zebbiche and Youbi, 2007) and (Raltson and Rabinowitz, 1985),

$$M(T) = \frac{\sqrt{2H(T)}}{a(T)} \quad (33)$$

With,

$$H(T) = \int_T^{T_0} C_P(T)\,dT \quad (34)$$

$$a(T) = \sqrt{\gamma(T)\ R\ T} \quad (35)$$

$$\gamma(T) = \frac{C_P(T)}{C_P(T) - R} \quad (36)$$

And,

$$\frac{\rho}{\rho_{0_2}} = \mathrm{Exp}\left(-\int_T^{T_0} \frac{C_P(T)}{a^2(T)}\ dT\right) \quad (37)$$

$$\frac{P}{P_{0_2}} = \left(\frac{T}{T_0}\right)\left(\frac{\rho}{\rho_{0_2}}\right) \quad (38)$$

The PG equation ($P=\rho RT$) remains valid, with R=287.102 J/(kgK). Expressions of $C_P(T)$ and R for air are presented in (Zebbiche and Youbi, 2007).

The values of (T_1/T_0, ρ_1/ρ_{01}, P_1/P_{01}) are constant and do not vary with β_i.

The third step consists in determining the flow properties (θ_S, M_2, ψ, T_2/T_1, ρ_2/ρ_1, P_2/P_1)$_i$ through the shock corresponding to each deflection β_i using the following oblique shock wave relationships at HT (Kenneth, 1996, 1997) and (Tatum, 1997),

$$\frac{\rho_2}{\rho_1} = \frac{\tan(\theta_S)}{\tan(\theta_S - \psi)} \quad (39)$$

$$\frac{T_2}{T_1} = \frac{\dfrac{\rho_2}{\rho_1} - M_1^2 \sin^2(\theta_S) \times \gamma(T_1) \times \left(1 - \dfrac{\rho_2}{\rho_1}\right)}{\left(\dfrac{\rho_2}{\rho_1}\right)^2} \quad (40)$$

$$\frac{P_2}{P_1} = \left[\frac{T_2}{T_1}\right]\left[\frac{\rho_2}{\rho_1}\right] \quad (41)$$

$$M_2^2 = \frac{1 - \dfrac{P_2}{P_1}}{\sin^2(\theta_S - \psi) \times \gamma(T_2) \times \left[1 - \dfrac{\rho_2}{\rho_1}\right]\dfrac{P_2}{P_1}} \quad (42)$$

Two solutions can be found according to the value of M_2, which implies that all the parameters will admit two solutions. If $M_2 \geq 1.00$, we get a weak shock. If $M_2 < 1.00$, we get a strong shock. Generally, the weak shock that occurs in the nature (Peterson and Hill, 1965) and (Zebbiche and Youbi, 2007).

The relation determining the analytical equation between (ψ, θ_S and M_1) does not exist. To determine the shock parameters by these relations, it is necessary first to determine the flow deviation ψ just after the shock. (Kenneth, 1996, 1997) and (Tatum, 1997) use the relation for a *PG* model at constant C_P, given the difficulty of finding an analytic form despite nonlinear, which gives the results are far from reality and does not respond to the *HT* model. Then our work, we will determine the deviation ψ with a high precision according to the real *HT* model. All the parameters after the shock depend in a direct and explicit way on ψ. Since there is a physical solution, the value of ψ must be greter than zero. As the development of an analytic relationship connecting θ_S and ψ is quite complicated, we will use the principle of a normal shock wave at *HT* to determine the value of M_2.

ISENTROPIC PARAMETERS JUST AFTER THE SHOCK

It is easy to determine the isentropic parameters T_2/T_0, ρ_2/ρ_{02} and P_2/P_{02}, immediately after the shock, corresponding to each longitudinal plane deviation number i by the relationships (33), (37) and (38) when ($M=M_2$, $T=T_2$, $\rho=\rho_2$ and $P=P_2$).

SHOCK INTENSITY

The total pressure ratio P_{02}/P_{01} for each deviation i can be determined by the following relation,

$$\left[\frac{P_{0_2}}{P_{0_1}}\right]_i = \frac{\left[\frac{P_2}{P_1}\right]_i \left[\frac{P_1}{P_{0_1}}\right]}{\left[\frac{P_2}{P_{0_2}}\right]_i} \tag{43}$$

The relation (43) will be used to determine the shock intensity expressed by the jump of entropie through the shock.

CONE SURFACE PARAMETERS

This step consists to find the isentropic flow parameters in the region just after the shock and the longitudinal surface, corresponding to the cone deflection β_i, by the numerical resolution of the coupled differential equations (44), (45) and (46) to three variables (V_r, V_θ and T) simultaneously by the use and adaptation of the Runge Kutta method of order 6 (Raltson and Rabinowitz, 1985), (Elaichi and Zebbiche, 2018) and (Curtis, 1975).

Figure 2 represents a general diagram of a conical shock wave with the physical parameters.

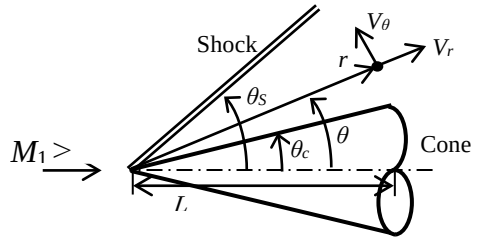

Fig. 2 Conical shock presentation

$$\frac{dV_r}{d\theta} = V_\theta \tag{44}$$

$$\frac{dV_\theta}{d\theta} = \frac{a(T)\left[2\,V_r\,tg(\theta)+V_\theta\right]-V_\theta^2\,V_r\,tg(\theta)}{tg(\theta)\left[V_\theta^2-a^2(T)\right]} \tag{45}$$

$$\frac{dT}{d\theta} = \frac{V_\theta\,a(T)\left[V_r\,tg(\theta)+V_\theta\right]}{tg(\theta)\,C_P(T)\left[a^2(T)-V_\theta^2\right]} \tag{46}$$

$$V^2 = V_r^2 + V_\theta^2 \tag{47}$$

$$V = \frac{M}{a} \tag{48}$$

In the relations (44)-(48), we need relationships (34)-(36). At each flow deflection θ just after the shock and the cone surface, the parameters a, M, ρ/ρ_{02} and P/P_{02} can be respectively determined by the relations (35), (48), (37) , (38).

Relationships (44), (45), (46), (47), (35), (48), (36) and (38) determine the isentropic flow parameters between the states just after the shock until the cone surface number i corresponding to the deflection β_i as a function of θ as shown in the figure 2. Then, since the cone surface deviation θ_C corresponding to the deflection β_i is known, we search the shock deviation θ_S. This deviation will be determined when the velocity V_θ for certain angle θ of the figure 2 will be zero.

By varying M_1, T_0 and β_i (i=1, 2, ..., N) and the shape of the cone cross section, we can find all the parameters θ_C, θ_S, ψ, M_2, T_2/T_1, ρ_2/ρ_1, P_2/P_1, P_{02}/P_{01}, T_2/T_0, ρ_2/ρ_{02}, P_2/P_{02}, M_C, T_C/T_0, ρ_C/ρ_{02}, P_C/P_{02}.

AERODYNAMIC COEFFICIENTS

The lateral surface of the cone is therefore divided into N triangles, limited with the nodes O, i and j, such that $j=i+1$ (i=1, 2, ..., N) as shown in the figure 3. If $i=N$ one have j=1.

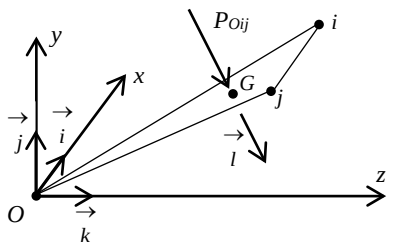

Fig. 3 Presentation of the elementary triangular surface

The pressure P_{Oij} applied to each elementary triangular surface is calculated as the average value at points *i* and *j* and it is applied on the center of gravity *G* of the triangle *Oij*, perpendicular and directed to the triangle surface in the direction of the unit vector $\vec{l}$ which is determined by the following relation,

$$\vec{l} = \frac{\vec{Oi} \wedge \vec{Oj}}{\left| \vec{Oi} \wedge \vec{Oj} \right|} \tag{49}$$

With,

$$\vec{Oi} \wedge \vec{Oj} = \left(y_i z_j - z_i y_j\right)\vec{i} + \left(z_i x_j - x_i z_j\right)\vec{j} + \left(x_i y_j - y_i x_j\right)\vec{k} \tag{50}$$

The position of the center of gravity *G* of the triangle *Oij* is given by,

$$x_{Oij} = \frac{x_i + x_j}{3} \ , \ y_{Oij} = \frac{y_i + y_j}{3} \ , \ z_{Oij} = \frac{z_i + z_j}{3} \tag{51}$$

The elementary force applied to the triangle *Oij* can be calculated by the following relation,

$$\vec{F}_{Oij} = P_{Oij} A_{Oij} \vec{l} \tag{52}$$

With,

$$P_{Oij} = \frac{P_i + P_j}{2} \tag{53}$$

And,

$$A_{Oij} = \frac{1}{2}\left| \vec{Oi} \wedge \vec{Oj} \right| \tag{54}$$

.

The pressure is calculated as a thermodynamic ratio. We calculated four ratios that are P_2/P_1, P_2/P_{02}, P_{02}/P_{01} and P_C/P_{02}. In the relation (52), we are interested on the pressure ratio on the cone surface $P_C/P_{02}=P_i/P_{02}=P_{Oij}/P_{02}$. Then, the pressure P_i can be calculated by the relation (55) since P_{02} is not constant after the shock. It depends on β_i,

$$P_i = \left(\frac{P_C}{P_{0_2}}\right)\left(\frac{P_{0_2}}{P_0}\right)_i P_0 \tag{55}$$

The pressure P_0 represents the total pressure at the upstream infinity. For external aerodynamic, P_0=total ambient pressure. For internal aerodynamic, P_0=total combustion chamber pressure.

Writing the relation (52) in the following form according to the global reference axes of the flow,

$$\vec{F}_{Oij} = X_{Oij}\,\vec{i} + Y_{Oij}\,\vec{j} + Z_{Oij}\,\vec{k} \tag{56}$$

Replace the relationships (6), (49) and (54) in the relation (52), we find,

$$X_{Oij} = \frac{1}{2} P_{Oij}\left(y_i z_j - z_i y_j\right) \tag{57}$$

$$Y_{Oij} = \frac{1}{2} P_{Oij}\left(z_i x_j - x_i z_j\right) \tag{58}$$

$$Z_{Oij} = \frac{1}{2} P_{Oij}\left(x_i y_j - y_i x_j\right) \tag{59}$$

The aerodynamic moment of the elementary force F_{Oij} with respect to the leading edge *O* can be calculated by the following relation,

$$\vec{m}_{Oij} = \vec{OG} \wedge \vec{F}_{Oij} \tag{60}$$

Replace relations (6), (49), (52) and (54) in relation (60), we find

$$\vec{m}_{Oij} = \left(y_{Oij} Z_{Oij} - z_{Oij} Y_{Oij}\right)\vec{i} + \left(z_{Oij} X_{Oij} - x_{Oij} Z_{Oij}\right)\vec{j} + \left(x_{Oij} Y_{Oij} - y_{Oij} X_{Oij}\right)\vec{k} \tag{61}$$

Consequently, the force exerted on the complete cone will be equal to the sum of all the elementary forces exerted on the surface of the *N* triangles. So,

$$\vec{F} = \sum_{\substack{i=1 \\ j=i+1 \\ If\ j=N,\ i=1}}^{i=N} \vec{F}_{Oij} = X\,\vec{i} + Y\,\vec{j} + Z\,\vec{k} \tag{62}$$

Likewise, the total moment exerted on the lateral cone surface is equal to the sum of all the elementary moments exerted on the *N* triangles. So,

$$\vec{m} = \sum_{\substack{i=1 \\ j=i+1. \\ If\ j=N,\ i=1}}^{i=N} \vec{m}_{Oij} = m_x \vec{i} + m_y \vec{j} + m_z \vec{k} \qquad (63)$$

In *Ox'y'z'*, we can write the following relations concerning the force and the aerodynamic moment, in the same way as the relations (62) and (63),

$$\vec{F}' = X' \vec{i}' + Y' \vec{j}' + Z' \vec{k}' \qquad (64)$$

$$\vec{m}' = m'_x \vec{i}' + m'_y \vec{j}' + m'_z \vec{k}' \qquad (65)$$

It is necessary to determine the inverse transformation from the *Ox'y'z'* reference to the *Oxyz* mark by expressing the unit vectors $\vec{i}$, $\vec{j}$, $\vec{k}$ as a function of $\vec{i}'$, $\vec{j}'$, $\vec{k}'$ directly from the relations (9). Then, we can determine the inverse of the orthogonal passage matrix [*A*]. Let us replace the relations (62) and (63) and identify the obtained result with relations (64) and (65) we obtain,

$$X' = A_{11} X + A_{21} Y + A_{31} Z \qquad (66)$$

$$Y' = A_{12} X + A_{22} Y + A_{32} Z \qquad (67)$$

$$Z' = A_{13} X + A_{23} Y + A_{33} Z \qquad (68)$$

$$m'_x = A_{11} m_x + A_{21} m_y + A_{31} m_z \qquad (69)$$

$$m'_y = A_{12} m_x + A_{22} m_y + A_{32} m_z \qquad (70)$$

$$m'_z = A_{13} m_x + A_{23} m_y + A_{33} m_z \qquad (71)$$

At the end, we can determine the 3 aerodynamic forces coefficients, and the 3 aerodynamic moment coefficients exerted on the complete surface of the cone, along the axes *Ox'*, *Oy'* and *Oz'* of the cone movement, by the following relations,

$$C_T = \frac{X'}{L^2 P_0} \quad , \quad C_L = \frac{Y'}{L^2 P_0} \quad C_D = \frac{Z'}{L^2 P_0} \qquad (72)$$

$$D_P = \frac{m'_x}{L^3 P_0} \quad , \quad D_Y = \frac{m'_y}{L^3 P_0} \quad D_R = \frac{m'_z}{L^3 P_0} \qquad (73)$$

RESULTS AND COMMENTS

Our applications will be presented for the consideration of 16 cross sections as shown in the figure 4. Some sections have axial symmetry such as circular section 16. Other sections have two symmetries with respect to the perpendicular axes such as sections 1, 2, 5 and 7. Other sections have symmetry with respect to a single axis such as sections 8, 9 and 11. The rest of the sections do not represent any symmetry. These sections can be considered as the random sections of complex geometries like sections 12, 13, 14, 15. The choice of these diversities of the sections is to represent the power of our developed numerical program.

Figure 5 represents the effect at *HT* on the variation of the physical parameters through the shock, and on the cone surface of the section 12 as a function of β when T_0=1000 K (curve 2), 2000 K (curve 3) and 3000 K (curve 4), including the *PG* model when γ=1.402 (curve 1), for M_1=3.00, α_x=90°, α_y=90°, α_z=0° only for weak shock. The angle β varies from 0° to 360° so that the physical parameter at β=0° is the same when β=360°. This figure represents that all the parameters depend on M_1, α_x, α_y, α_z, T_0 and β. The difference between the flow around a 3D cone of arbitrary cross section (our study) and the flow around cone of circular section (section 16 (Elaichi and Zebbiche, 2018)) is that this section, the parameters do not depend on β. Whreas for our case, the parameters depend on β. This result demonstrates that the flow around a circular cone is a quasi-3D flow (1D computation and 3D presentation (Elaichi and Zebbiche, 2018)) because the flow depends solely on the space variable θ of the figure 2. While our problem is really of 2D type since it depends on the two space variables (θ and β). The presentation is only 3D.

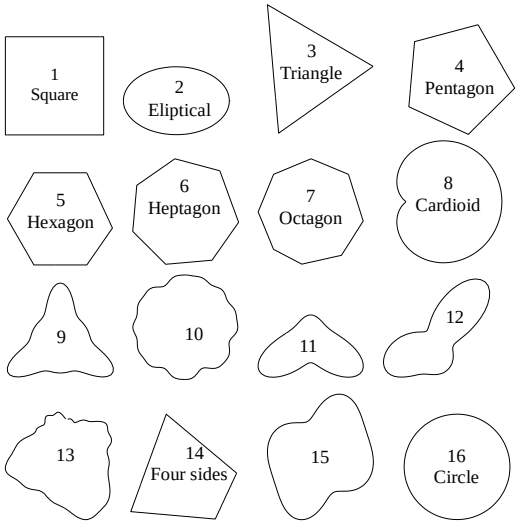

Fig. 4 Various shapes of 3D cone cross sections

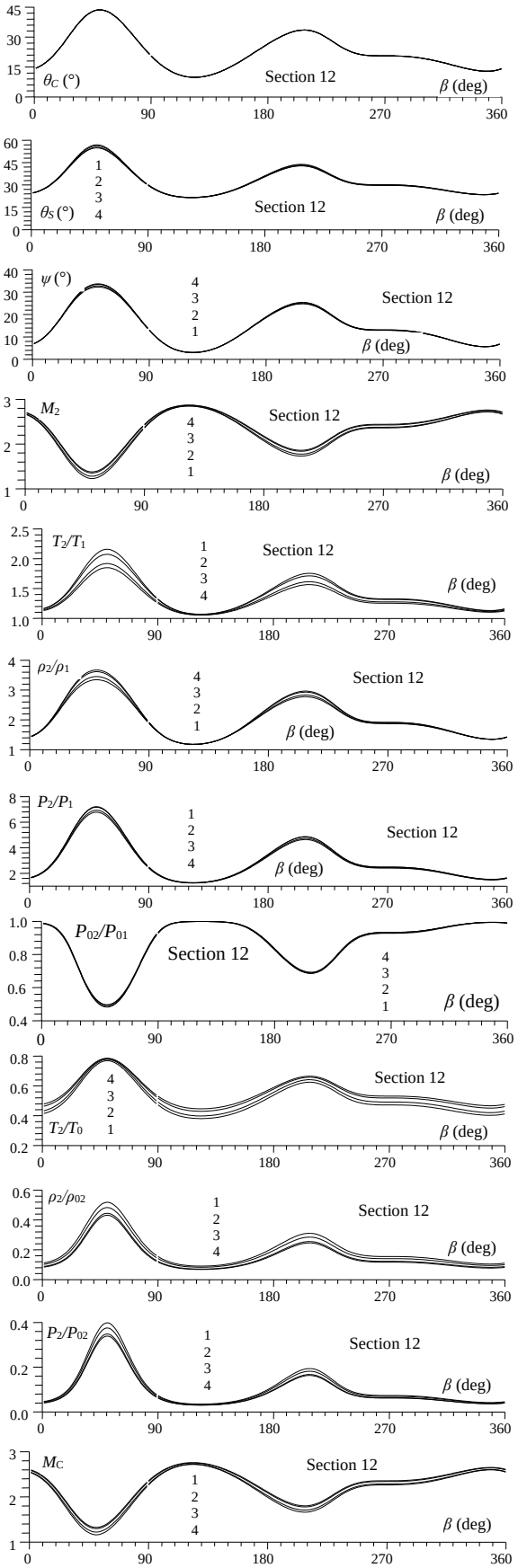

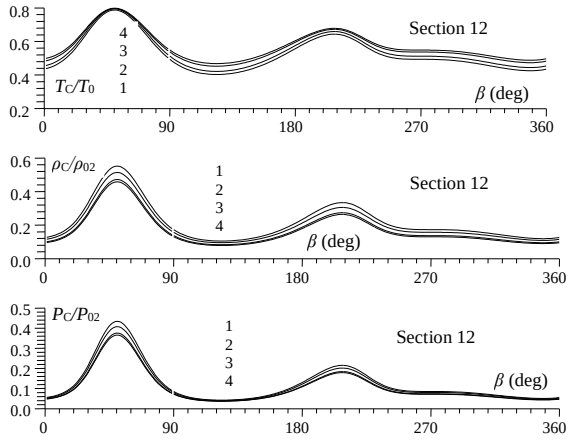

M_1=3.00, α_x=90°, α_y=90°, α_z=0°.
Curve 1 : *PG* (γ=1.402). Curve 2 : *HT* (T_0=1000 K)
Curve 3 : *HT* (T_0=2000 K). Curve 4 : *HT* (T_0=3000 K)

Fig. 5 Effect of T_0 on the variation of the flow parameters around a cone of section 12 as a function of β.

In the figue 6, the presentation is limited only to M_C as a function of β for the 16 chosen sections when M_1=3.00, α_x=90°, α_y=90°, α_z=0°. The presentation is made again at *HT* for T_0=1000 K, (curve 2), T_0=2000 K (curve 3), T_0=3000 K (curve 4), including the *PG* model (curve 1). The figure represents the results only for the weak shock. The influence of the shape of the cross section on M_C variation, and therefore on all other physical parameters is clearly noticeable. On the circular section 16, it is clearly seen that the M_C does not depend on β which demonstrates that there is only a single value of M_C on the cone surface, which is not the case for any other sections some is its geometric form. The result of the section 16 is the purpose of the reference (Elaichi and Zebbiche, 2018).

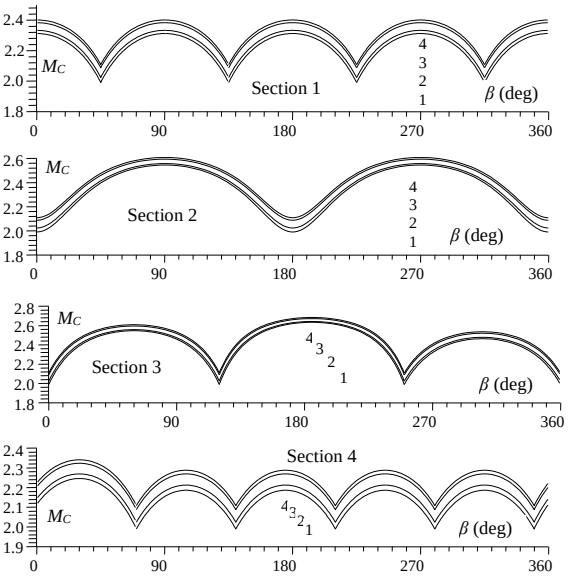

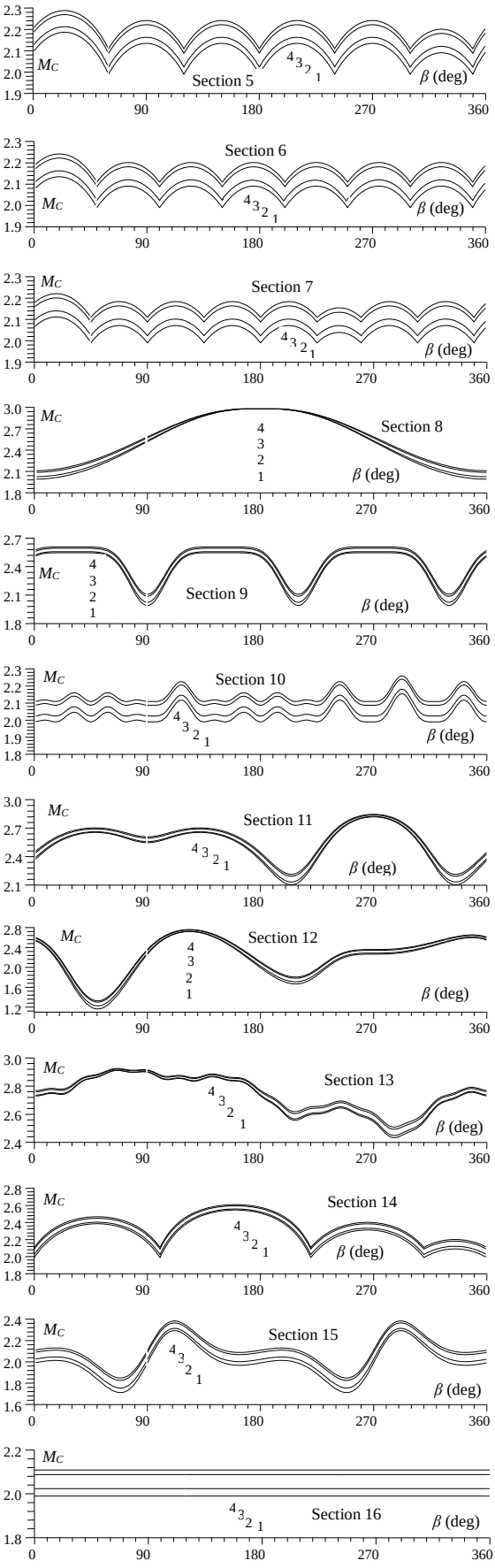

M_1=3.00, α_x=90°, α_y=90°, α_z=0°.

Curve 1 : *PG* (γ=1.402). Curve 2 : *HT* (T_0=1000 K)
Curve 3 : *HT* (T_0=2000 K). Curve 4 : *HT* (T_0=3000 K)

Fig. 6 Effect of T_0 on the M_C variation for of the 16 different sections as a function of the angle β.

In figure 7, we presents the M_1 effect on the variation of the physical parameters for the section 12 as function of β, when T_0=2000K, α_x=90°, α_y=90° and α_z=0°. The 4 curves show respectively the parameters variation for M_1=3.00 (curve 1), M_1=4.00 (curve 2), M_1=5.00 (curve 3) and M_1=6.00 (curve 4). It is noted that M_1 mainly affects all the parameters in addition to the influence of T_0, α_x, α_y and α_z. The results presented are for the weak shock. Curve 1 in the figure 7 represents curve 3 in the figure 5.

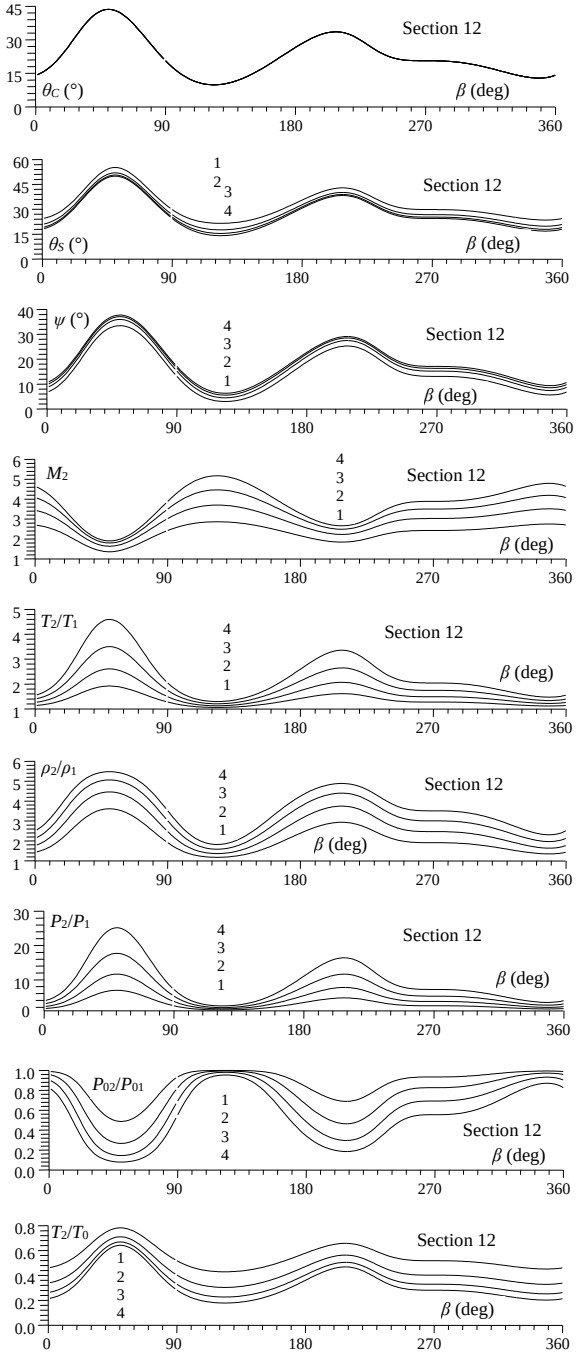

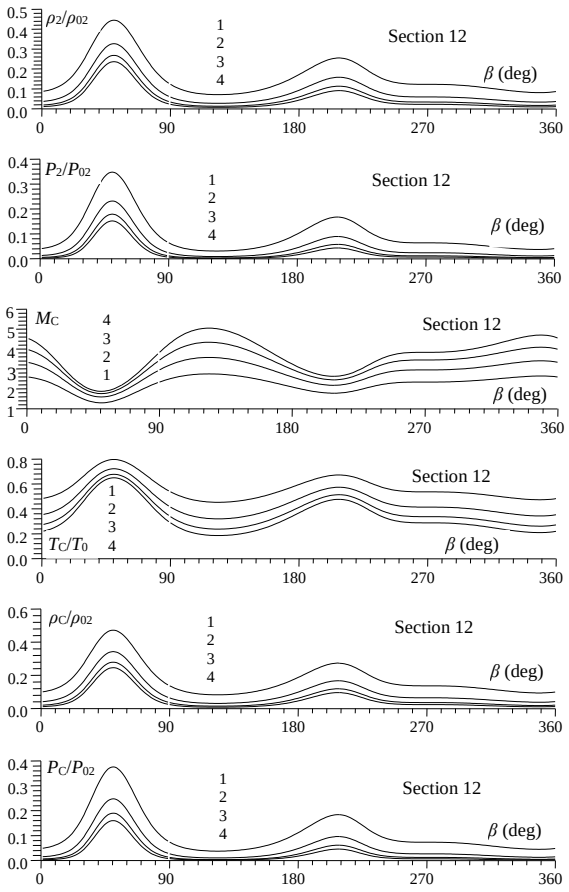

T_0=2000 K, α_x=90°, α_y=90°, α_z=0°.
Curve 1 : M_1=3.00. Curve 2 : M_1=4.00.
Curve 3 : M_1=5.00. Curve 4 : M_1=6.00.

Fig. 7 Effect of M_1 on the variation of the flow parameters around the cone of section 12 versus β.

Among all the flow parameters, it has been chosen to present in the figure 8 the effect of M_1 and the shape of the cross-section on M_C as a function of β. The results are chosen for T_0=2000 K, α_x=90°, α_y=90°and α_z=0°. The 4 curves show respectively the variation of M_C for M_1=3.00 (curve 1), M_1=4.00 (curve 2), M_1=5.00 (curve 3) and M_1=6.00 (curve 4). It is noteworthy that M_1 mainly influences M_C in addition to the effect of T_0, α_x, α_y and α_z. The results presented are for the weak shock. The curve 1 in figure 8 represents the curve 3 in figure 6. On the circular section 16, it is clearly seen that the M_C does not depend on β. This result demonstrates that there exists only a single value of M_C on the cone surface, which is not the case for any other sections whatever its geometric shape. The variation shown in section 16 is the purpose of (Elaichi and Zebbiche, 2018).

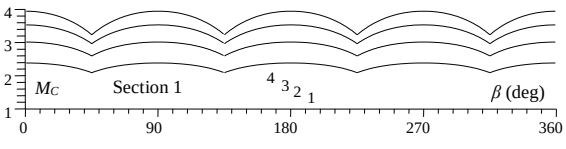

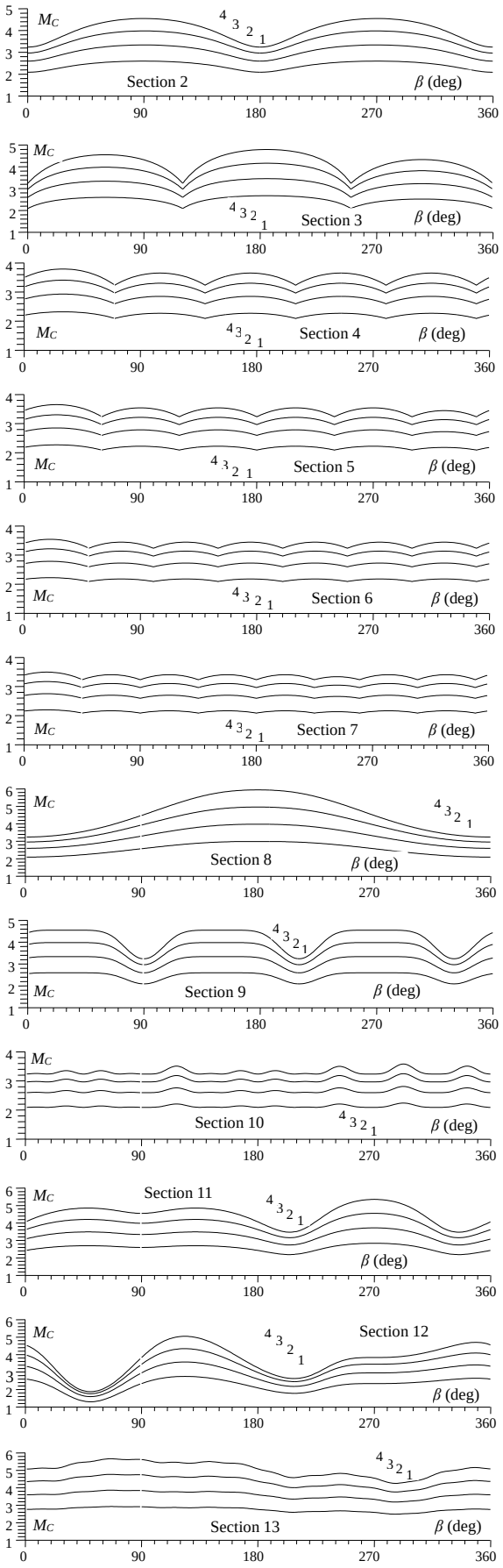

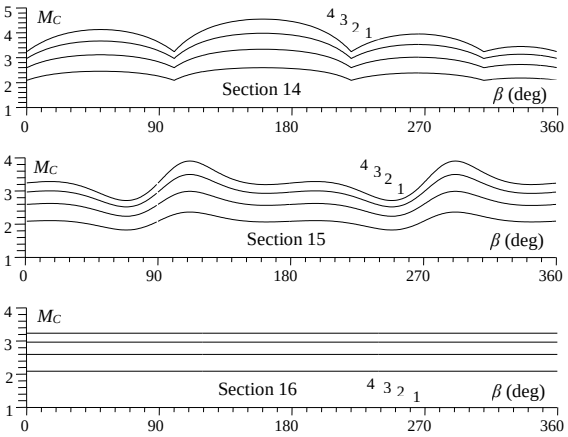

T_0=2000 K, α_x=90°, α_y=90°, α_z=0°.
Curve 1 : M_1=3.00. Curve 2 : M_1=4.00.
Curve 3 : M_1=5.00. Curve 4 : M_1=6.00

Fig. 8 Effect of M_1 on the M_C variation of the different sections as a function of β.

Figure 9 represents the angle incidence effect, and the shape of the cross section on the variation of the physical parameters of the section 12 as a function of β. The results are chosen for M_1=3.00 and T_0=2000 K. The 4 curves respectively show the variation for (α_x=90°, α_y=90°, α_z=0°) (blue curve), (α_x=89°, α_y=89°, α_z=1°) (red curve), (α_x=85°, α_y=85°, α_z=3°) (black curve) and (α_x=80°, α_y=80°, α_z=12°) (purple curve). It is noted that the incidence angle influences mainly all the physical parameters. The results are presented for the weak shock. The blue curve in figure 9 represents the curve 1 in the figure 7.

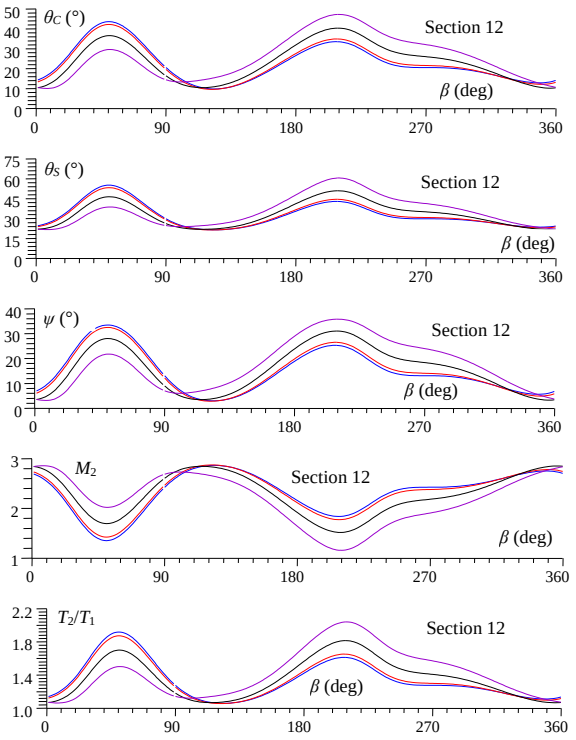

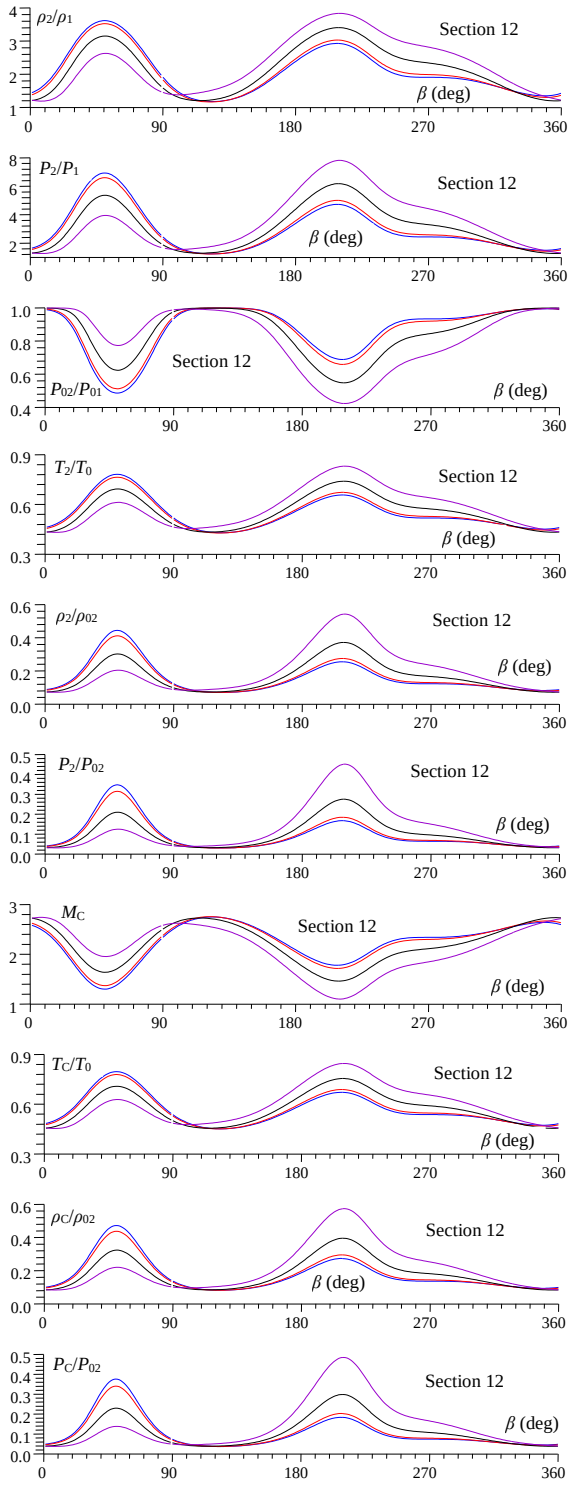

M_1=3.00, T_0=2000 K.
: α_x=90°, α_y=90°, α_z=0°
: α_x=89°, α_y=89°, α_z=1°
: α_x=85°, α_y=85°, α_z=3°
: α_x=80°, α_y=80°, α_z= 12°

Fig. 9 Effect of incidence angle on the variation of the flow parameters around the cone of section 12 versus β.

Figure 10 shows the incidence angle and the shape of the cone cross-section effect on the M_C as a function of β when M_1=3.00 and T_0=2000 K. The

figure contains 4 curves. The curve in blue shows the variation of M_C when α_x=90°, α_y=90°, α_z=0°. The curve in red is for α_x=89°, α_y=89°, α_z=1°. The curve in black is for α_x=85°, α_y=85°, α_z=3°. The purple curve is for α_x=80°, α_y=80°, α_z=12°. The infiuence of α and the shape of the cross-section on M_C variation are clearly noticeable. For the circular section 16, one always notices that the M_C does not depend on β when α_x=90°, α_y=90 °, α_z=0°, which is the aim of (Elaichi and Zebbiche, 2018). But when α changes value, we notice that there is a variation of M_C with β for all sections including the section 16, and consequently all the other physical parameters vary with β. The blue curve in the figure 10 shows the curve 1 in the figure 8 for comparison.

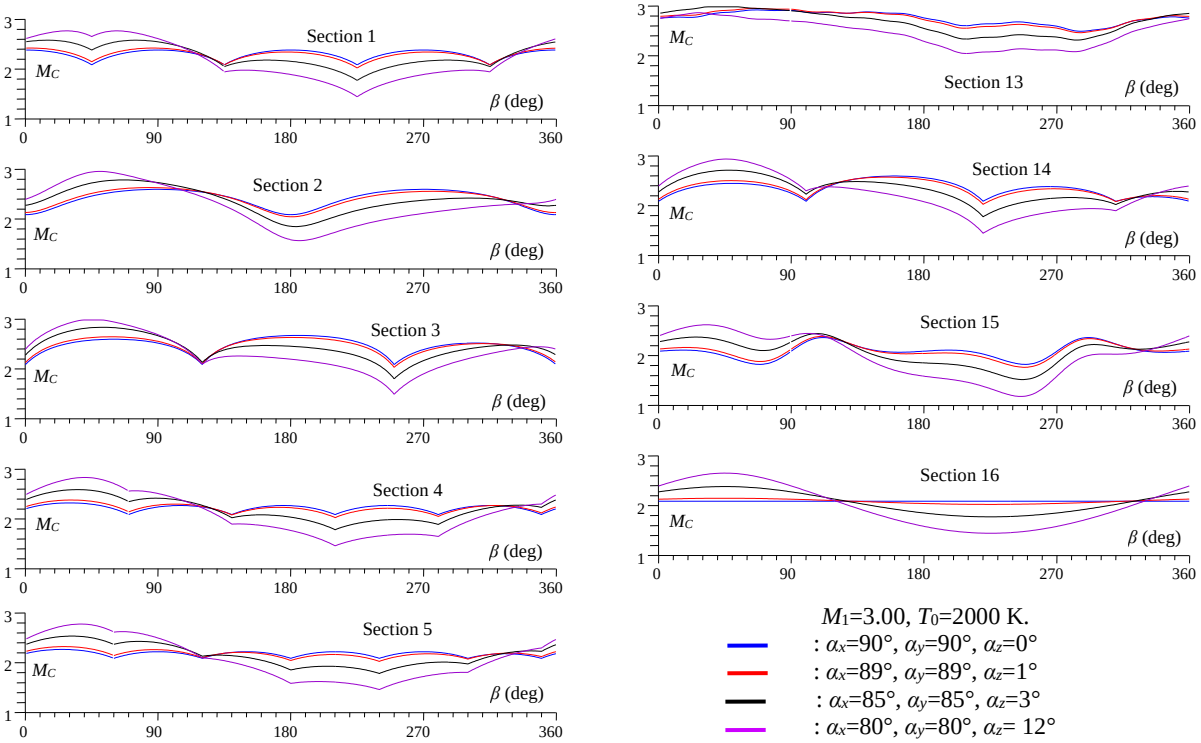

Fig. 10 Effect of α on M_C variation for the different sections as a function of β.

Given the present work is done for the calculation of the supersonic flow parameters, it is very important to complete it by the calculating the variation of the aerodynamic coefficients. The shape of the cross section has shown that there are 6 aerodynamic coefficients along the 3 axes of flight. Three are designed for the aerodynamic force and three for the aerodynamic moment.

The results on the tables 1, 2 and 3 are shown only for the section 12 as a typical example of a complex 3D section.

In the table 4, we presented the effect of M_1, T_0 and α on the 6 aerodynamic coefficients of all the sections chosen in this study.

On the table 1, we clearly see the T_0 effect to HT on the 6 coefficients. Likewise, in the tables 2 and 3,

the effect of M_1 and α on the aerodynamic coefficients are respectively noted.

Table 1 : T_0 effect on the 6 aerodynamic oefficients of section 12 for M_1=3.00 and α_x=85°, α_y=85°, α_z=3°

	PG (γ=1.402)	*HT* T_0=1000 K	*HT* T_0=2000 K	*HT* T_0=3000 K
C_T	-0.00139	-0.00127	-0.00106	-0.00097
C_L	0.01023	0.00968	0.00878	0.00849
C_D	0.09399	0.08901	0.08098	0.07840
D_P	-0.01177	-0.01114	-0.01011	-0.00977
D_T	0.00200	0.00194	0.00184	0.00183
D_R	0.00024	0.00019	0.00014	0.00011

Table 2 : M_1 effect on the 6 aerodynamic coefficients of section 12 for T_0=2000 K, α_x=85°, α_y=85°, α_z=3°

	M_1=2.00	M_1=3.00	M_1=4.00	M_1=5.00	M_1=6.00
C_T	0.00073	-0.00106	-0.00068	-0.00035	-0.00018
C_L	0.02633	0.00878	0.00313	0.00129	0.00060
C_D	0.25595	0.08098	0.02803	0.01135	0.00524
D_P	-0.03027	-0.01011	-0.00360	-0.00148	-0.00069
D_T	0.00882	0.00184	0.00040	0.00010	0.00003
D_R	0.00038	0.00014	0.00011	0.00006	0.00003

Table 3 : Effect of (α_x, α_y, α_z) on the 6 aerodynamic coefficients of section 12 for M_1=3.00, T_0=2000 K.

	α_x=90° α_y=90° α_z=0°	α_x=87° α_y=87° α_z=2°	α_x=85° α_y=85° α_z=3°	α_x=80° α_y=75° α_z= 12°
C_T	-0.00432	0.00349	-0.00106	-0.00386
C_L	-0.01171	0.00937	0.00878	-0.00512
C_D	0.08440	0.08149	0.08098	0.08750
D_P	0.02441	-0.01137	-0.01011	0.01539
D_T	-0.01262	0.01133	0.00184	-0.01539
D_R	0.00000	-0.00034	0.00012	0.00101

Table 4 : Aerodynamic coefficients of the 16 sections when M_1=3.00, T_0=2000 K, (α_x=85°, α_y=85°, α_z=3°)

S	C_T	C_L	C_D	D_P	D_T	D_R
1	-0.0110	-0.0036	0.0403	0.0053	-0.0111	0.0004
2	-0.0087	-0.0036	0.0304	0.0040	-0.0088	0.0004
3	-0.0062	-0.0046	0.0224	0.0052	-0.0055	0.0002
4	-0.0134	-0.0039	0.0517	0.0065	-0.0142	0.0006
5	-0.0136	-0.0043	0.0584	0.0075	-0.0148	0.0006
6	-0.0141	-0.0038	0.0632	0.0073	-0.0158	0.0006
7	-0.0144	-0.0039	0.0662	0.0077	-0.0164	0.0007
8	0.0078	-0.0080	0.0206	0.0085	0.0081	0.0003
9	-0.0082	-0.0028	0.0257	0.0037	-0.0077	0.0003
10	-0.0139	-0.0029	0.0698	0.0067	-0.0162	0.0007
11	-0.0072	-0.0062	0.0159	0.0058	-0.0064	0.0003
12	-0.0010	0.0087	0.0809	-0.0101	0.0018	0.0001
13	-0.0038	-0.0037	0.0061	0.0033	-0.0031	0.0001
14	-0.0049	-0.0100	0.0303	0.0113	-0.0040	0.0001
15	-0.0076	-0.0032	0.0222	0.0033	-0.0072	0.0003
16	-0.0023	0.0019	0.0028	-0.0016	-0.0019	0.0001

Table 4 shows a typical example of the calculation of the 6 aerodynamic coefficients of the 16 selected sections when T_0=2000, M_1=3.00 and (α_x=85°, α_y=85° and α_z=3°). This table presents the effect of the 3D cross-section on the 6 coefficients. One can choose consequently the suitable form according to our need.

Table 1 represents the difference between the *PG* and *HT* model on the variation of the 6 aerodynamic coefficients. The variation is made as a function of T_0 when M_1=3.00 and α_x=90°, α_y=90°, α_z=0°. The *PG* model does not depend on T_0 and can be assimilated as *HT* model for low T_0<240 K. We note again that the *HT* model is destined to make corrections to the *PG* model when T_0>240 K. We can say that our *HT* model is a generalization of the *PG* model when T_0 will be raised.

Tables 1, 2, 3 and 4 clearly represent the effect of M_1, T_0, α and the shape of the transeversal cone section on the values of the 6 aerodynamic coefficients which demonstrate that there is a strong maneuverability during the flight according to the 3 directions since the 6 coefficients are not zero.

CONCLUSIONS

From this study, we can quote the following conclusions:

1. The developed program can process any cross section of the 3D cone. Te presentation is limited by 16 cross-sections.
2. T_0 is an essential parameter of our *HT* model. The *PG* model results do not depend on T_0.
3. T_0 degrades the parameters θ_S, T_2/T_1, P_2/P_1, ρ_2/ρ_{02}, P_2/P_{02}, ρ_C/ρ_{02}, P_C/P_{02} and increases the parameters M_2, ψ, ρ_2/ρ_1, P_{02}/P_{01}, T_2/T_0, M_C, T_C/T_0 with respect to the results of the *PG* model and this difference increases with the increase of T_0.
4. The flow around a cone of circular cross section really depends on one space variable (1D) which is θ and does not depend on β. While the flow around an arbitrary 3D cross section cone depends on two space variables (2D) that are θ and β. The presentation is only 3D.
5. The flow around a cone of circular cross section with zero incidences becomes a particular case of our modest work.
6. The *PG* model gives good results if M_1<2.00, T_0<240 K and θ_C<20°.
7. If M_1>2.00 or T_0> 240 K or θ_C>20°, the correction of the *PG* model results is necessary, which gives the needs to use our *HT* model.
8. The supersonic flow around a cone of arbitrary cross section is characterized by strong flight maneuverability, since there are 6 aerodynamic coefficients in the 3 flight directions.
9. The 6 aerodynamic coefficients presented in this work are only those given by the shock wave.
10. For low M_1 approaching to unity, there is the limit of having a detached shock wave. This size depends on the shape of the cone (that is to say of θ_C) as well as on the values of T_0, α_x, α_y and α_z.

As a perspective, the supersonic flow around a cone of arbitrary cross section and *curved* with the longitudinal direction at *HT* can be studied. In this case one will have the birth of a progressive shock and or a progressive Prandtl Meyer expansion. The flow in this case is actually of three-dimensional calculation, where it depends on three space variables (θ, β, z).

REFERENCES

Amidon P. F., "Supersonic Aerodynamic Characteristics of Elliptic Cross-Section Bodies," AIAA Paper No.1607-1985, (1985).

Briggs B. R., "The Numerical Calculation of Flow Past Conical Bodies Supporting Elliptic Conical Shock Waves at Finite Angles of Incidence," NASA TN D-340, (1960).

Chen S. X. and Li D. N., "Supersonic flow past a symmetrically curved cone," Indiana University Mathematical Journal, Vol. 49, PP. 1411-1435, (2000).

Curtis A. R., "High-ordre Explicit Runge Kutta Formulae. Their Uses, and Limitations. Journal Institute Mathematical Applied, Vol. 16, PP. 35-55, (1975).

Eastman E. W., and Omar M. E., "Flow Fields About Highly Yawed Cones by the Inverse Method," AIAA Journal, Vol. 3, N° 9, PP. 1782-1784, (1965).

Elaichi T. and Zebbiche T., "Stagnation temperature effect on the conical shock with application for air," Chinese Journal of Aeronautics, Vol. 31, N° 04, PP. 672-697, (2018).

Goldsmith E. L. and Seddon J., "Intake Aerodynamics," Blackwell Science, Second Edition, (1999).

Kenneth E. T., "Computation of thermally perfect properties of oblique shcok waves," NASA CR-4749, (1996).

Kenneth E. T., "Computation of thermally perfect oblique shcok waves properties," AIAA-97-0868, 35th Aerospace Sciences Meeting and Exhibit, Aerospace Sciences Meetings, 06-09 January (1997).

Kopal Z., "Tables of Supersonic Flow Around Cones," Massachusetts Institute of Technology, Dept. of Electrical Engineering Tech. Report No. 1, Cambridge, Mass., (1947).

Kopal Z., " Tables of Supersonic Flow Around Cones of Large Yaw," Massachusetts Institute of Technology, Dept. of Electrical Engineering, Tech. Report No. 5, Cambridge, Mass., (1949).

Maccoll J. W., "The conical shock wave formed by a cone moving at high speed," Proceddings of the Royal Soceity of London A, N° 159, PP. 459-472, (1937).

Maslen S. H., "Supersonic Conical Flow," NACA TN 2651, (1952).

McBride B. J., Gordon S. and Reno M. A., "Coefficients for Calculating Thermodynamic and Transport Properties of Individual Species," NASA TM 4513, (1993).

Ndefo D. E., "A Numerical Method for Calculating Steady Unsymmetrical Supersonic Flow Past Cones," Rep. No. AS-69-11 (AFOSR Grant 268-68), U.S. Air Force, May 1969.

Peterson C. R. and Hill P. G., "Mechanics and Thermodynamics of Propulsion," Addition-Wesley Publishing Company Inc., New York, USA, (1965).

Raltson, A. and Rabinowitz A., "A First Course in Numerical Analysis," McGraw Hill Book Company, (1985).

Sims J. L., "Tables for Supersonic Flow Around Right Circular Cones at Zero Angle of Attack," NASA SP-3004, (1964).

Tatum K. E., "Computation of Thermally Perfect Oblique Shock Wave Properties," 35th Aerospace Sciences Meeting and Exhibit, Reno, AIAA-97-0868, (1997).

Zebbiche T. and Youbi Z., "Effect of stagnation temperature on the supersonic flow parameters with application for air in nozzles," The Aeronautical Journal, Vol. 111, N° 1115, PP. 31–40, (2007).

Zebbiche T., "Effect of Stagnation Temperature on the Normal Shock Wave," International Journal of Aeronautical and Space Sciences, Vol. 10, N° 01, PP. 1-14, (2009).

NOMENCLATURE

M	Mach number.
V	Velocity
ρ	Density
P	Pressure
T	Temperature
ψ	Flow deflection just after the shock
a	Sound velocity
H	Enthalpy
R	Thermodynamic constant of air
γ	Specific heats ratio
θ_C	Cone surface deviation
θ_S	Conical shock deviation
α_x	Angle of incidence between M_1 and the Ox axis
α_y	Angle of incidence between M_1 and the Oy axis
α_x	Angle of incidence between M_1 and the Oz axis
v_x	Angle of incidence around the Ox axis
v_y	Angle of incidence around the Oy axis
v_x	Angle of incidence around the Oz axis
F	Aerodynamic force in the $Oxyz$ mark
X	Aerodynamic force along the Ox axis
Y	Aerodynamic force along the Oy axis
Z	Aerodynamic force along the Oz axis
F'	Aerodynamic force in the $Ox'y'z'$ mark
X'	Aerodynamic force along the Ox' axis
Y'	Aerodynamic force along the Oy' axis
Z'	Aerodynamic force along the Oz' axis
G	Center of gravity of an elemental triangle
N	Number of points of the cone cross section.
m	Aerodynamic moment relative to the cone leading edge in the $Oxyz$ mark
m_x	Aerodynamic moment around the Ox axis
m_y	Aerodynamic moment around the Oy axis
m_z	Aerodynamic moment around the Oz axis
m'	Aerodynamic moment relative to the cone leading edge in the $Ox'y'z'$ mark
m'_x	Aerodynamic moment around the Ox' axis
m'_y	Aerodynamic moment around the Oy' axis
m'_z	Aerodynamic moment around the Oz' axis
C_T	Trigger force coefficient
C_L	Lift force coefficient
C_D	Drag force coefficient
D_P	Pitchnig moment coefficient
D_Y	Yaw moment coefficient
D_R	Roullette moment coefficient
$[A]$	Matrix of passage

β	Polar deviation of the cone cross section surface.
r	Polar Ray
z	Longitudinal abscissa of cone
x, y	Position of a point in the cone cross-section.
θ	Flow angle deviation.
l	Normal unit vector to the cone surface
L	Longitudinal length of the cone
HT	High Temperature
PG	Perfect Gas
C_P	Specific heat at constant pressure
f_1, f_2, f_3	Nonlinear equations
i, j, k	Angles for calculating f_1, f_2 and f_3
l	To divide 360 degrees into 4 quadrants

Subscripts

1	Upstream shock condition
2	Downstream shock condition
0	Stagnation condition
C	Cone surface parameter
θ	Cross-sectional component
r	Radial component
O	Benchmark position
S	Shock
Oij	Triangular elementary surface
x	Ox axis
y	Oy axis
z	Oz axis